Future Changes in Global Land Use Emissions

By
Farzad Taheripour[†*], Xiaojuan Yang[*], and Atul Jain[*]

January 2007

10th Annual Conference on Global Economic Analysis
University of Purdue
West Lafayette, IN
June 7-June 9, 2007

[*] Department of Atmospheric Science, University of Illinois at Urbana Champaign
[†] Now at Department of Agricultural Economics, Purdue University

Abstract

The objective of this paper is to evaluate the potential contribution of regionally-specific land use-related activities to the future emissions at 0.5^o x 0.5^o resolution. We have developed a downscaling framework, which spatially disaggregates future land uses changes based on socio-economic, biophysical, and biogeochemical factors at 0.5^o by 0.5^o resolution. The downscaling framework has been used to calculate greenhouse gas emissions for two IPCC scenarios, A2 and B2. Results indicates that Land uses changes under the A2 scenario contribute significantly to the emissions of CO_2, CO, NOx, and NMHCs. Under this scenario land use changes generate 0.8 Gt/yr CO_2, 71.1 Tg/yr CO, 1.9 Tg/yr No_x, and 4.9 Tg/yr NMHCs by 2025, which drop to 0.6 Gt/yr, 16.5 Tg/yr, 0.4 Tg/ye, and 1.0 Tg/yr by 2050. Results also indicate that more land will be available for the Agro-Ecological zones, which represent a length of growing period between 120 to 239 days in the future under both scenarios.

1. Introduction

Human activities are important source of greenhouses gases (GHGs) (CO_2, CH_4, and N_2O), reactive GHGs (CO, NOx), and non-methane hydrocarbon compounds (NMHCs). These gases and their interactions can impact the climate system. Although fossil fuels are major sources of theses gases, other sources such as land use changes, biomass burning, soil decomposition, oceans, and non-vehicle mobile sources are also contribute to theses emissions. Houghton (2003) estimates that about one third of total emissions of carbon into the atmosphere since 1850 has resulted from land use change. Jain et al. (2006) have shown that land use changes for croplands are also the major sources of CO, NO, and NMHCs emissions.

Given the significant contributions of land use changes to these gases and their future trends, accurate estimates of future emissions from land use changes is a vital task. Emissions of GHGs and reactive GHGs due to land use changes mainly come from converting natural land cover for agricultural land and other types of land uses. Changes in land use and land cover, biophysical factors, climate conditions, and human activities are linked together in a complex way. Land use activities contribute to climate change and humans change land use to adjust to climate change. Hence, one needs to consider ecosystem processes, economic models and demographic factors in prediction of emissions due to land use and land use changes.

While biophysical models have integrated climate and land use changes to project historical land use emissions at a grid level (Eickhout et al., 2008; Jain and Yang, 2005; Rounsevell et al., 2005; Tian et al., 1999; Feddama et al., 2005; and Rotmans et al., 1990)., there are still relatively few modeling analyses of future emissions scenarios that include land use change at a grid level[1], which are crucial to study the future impacts of climate change using Atmosphere-Ocean General Circulation Models (A-OGCMs). IPCC analyses, including the Special Report on Emissions Scenarios (Nakicenovic and Sward, 2000), have developed land use change scenarios at regional level. A few studies have predicted the impacts of land use changes at a grid level by spatially disaggregating IPCC regional changes in land cover, and other activities (Rounsevell et al., 2005; Feddama et al., 2005).

[1] Examples are: Rounsevell et al., 2005; Feddama et al.; 2005; and Rokityanskiy et al., 2006

The objective of this paper is to evaluate the potential contribution of regionally-specific land use-related activities, such as cropping and urbanization, to the future emissions of GHGs and reactive GHGs at a 0.5^o by 0.5^o resolution. To achieve this goal, we have developed a framework, which spatially disaggregate future changes in land cover, and other activities at 0.5^o by 0.5^o resolution. Next, the emissions are calculated using downscaling framework in combination with the biophysical component of the ISAM model and regional land use changes for two IPCC scenarios, A2 and B2, calculated based on the Mini Climate Change Assessment Model (MiniCAM). These scenarios cover two extreme cases of population growth.

The paper is organized as follow: Section 2 describes models which either used or developed in the paper. Section 3 explains data used in this study. Section 4 presents land use results for scenarios A2 and B1. Finally, section 5 provides the conclusion.

2. Methods

2.1. Downscaling Method

The spatial distribution of land use changes is an important factor which can affect the land use emissions estimates, significantly. For example, the additional need for cropland in a region can be obtained either from cutting down forests or disturbing other natural vegetation areas. These two alternatives have different emissions consequences. Therefore, to reduce uncertainty in land use emission estimates, it is important to determine grided specific land use changes within a region. Since biophysical, biogeochemical, and socio-economic factors are the key items which can affect distribution of land use changes within a region in the future, we build a downscaling method based on future changes in these factors. As a first step, we assume that the most profitable land in terms of production should be taken into account to grow crops. To determine the productivity of land we use biophysical and biogeochemical factors for each grid cell. Second, we introduced economic factors into framework. We rank each factor between 0 and 1. Then we combine ranking of all factors for each grid zone. Finally, we allocate changes in the regional demand between grid zones according to their ranks. In this process the most profitable land goes into production first. For those cases where there is a reduction in the regional demand for cropland, we take off the least productive cropland first.

Next we describe biophysical, biogeochemical, and socio-economic factors considered in this study.

2.1.1. Biophysical and Biochemical Factors

We measure productivity of land by using the concept of the Length of Growing Period (LGP). The LGP refers to the period during the year when both soil moisture and temperature are conducive to crop growth (Fischer et al., 2000 and 2002). The LGP is function of climate conditions, soil conditions and properties, and water availability. Here we implement LGP algorithm into biophysical and biogeochemical cycle components of the ISAM (Jain and Yang, 2005) to determine the LGP for each grid zone for 2000-2050. The ISAM biogeochemical cycles consist of fully prognostic carbon and nitrogen dynamics associated with vegetation, litter (above and below ground) decomposition, and soil organic matter. The ISAM biophysical model accounts for water and energy processes in vegetation and soil column. The ISAM model simulates the carbon and nitrogen fluxes to and from different compartments of the terrestrial biosphere with 0.5-by-0.5 degree spatial resolution. A schematic diagram of the terrestrial ecosystem component of the ISAM is presented in figure 1. The description of the carbon cycle component and subsequent examination of the regional and global pattern of carbon sources and sinks implied by land use changes, climate, and CO2 have been described in detail in Jain and Yang (2005). The ISAM model also consists of forest clearing and agriculture waste reservoirs. The carbon stored in these reservoirs is released to the atmosphere at a variety of rates depending on usage and is assigned products into three general reservoirs with turnover time of 1 year (agriculture and agriculture products), 10 years (paper and paper products), and 100 years (lumber and long lived products). These reservoirs allow us to account for biomass burned through land transformation (Jain et al., 2006).

In some part of the world land productivity, in terms of LGPs, relies on the irrigation facilities[2]. In those areas, the model calculated LGPs accounts for the amount of land irrigated. The LGP is an indication of land productivity, but in some places even with a high LGP, the land is not suitable for cropping practices due to the terrain conditions. Hence, we define an index

[2] For the irrigation data source see section 3 of this paper.

which measures the terrain slope of the land for each grid zone[3]. Then we combine the LGP index with the terrain slope index to appreciate lands with high LGP and low terrain slope.

2.1.2. Economic Factors

Since prediction of economic factors such as prices and costs is not a feasible practice at the grid zone level, we use a set of indices to indirectly account for economic factors into the framework. The history of land use of a grid point can provide valuable information about cropping practices at that point. For example, an increasing trend in the share of cropland in total area of a grid zone indicates that cropping practices have been attractive in that grid zone in the past. The increasing trend in the share of croplands in a grid zone can be a sign of economic advantages (in terms of cropping activities) for that grid zone compared to other grid zones which may experienced a reduction in the share of croplands. For this reason we define an index which measures the history of cropping activities in each grid zone[4]. We construct this index based on the changes in the share of crop land in the past 10 years. The index appreciates grid zones which have experienced an increasing trend in their croplands.

In addition to the history of land use, the current distribution of land can carry some economic information as well. For example, we can expect that in a grid zone where crop production is the major activity and the infrastructure supports agricultural activities, it is less costly to expand cropping activities compared to the grid zones which are not involved in crop production. Hence we construct another index which appreciates grid zones with higher cropland shares. However, we exclude grid zones with a cropland share more than 90 percent to avoid high marginal costs. Finally, in our downscaling method we define a priority index which assigns points to each grid zone based on the current cropping activities in their neighbor cells. We appreciate gird zones which have neighbors with high ratio of cropland.

[3] For the terrain slope data source see section 3 of this paper.
[4] Verburge et al. (1999) have developed a statistical framework to predict future land use at the grid zone level, based on the history of land use. They applied their model to simulate land use scenarios for Ecuador. While this model is suitable for small regions, it is not practical to use their model for the whole world due to the lack of data.

2.2. Future Demand for Cropland and Urban Land

We use regional land use projections provided by the MiniCam, a long-term, partial-equilibrium model of the energy, agriculture, and climate system developed at the Pacific Northwest Laboratory (PNL)[5]. The model has the capability to predict future regional land use changes based on the climate and socio-economic factors. Figures 2 panels (a) and (b) depict MiniCAM estimates for changes in the demand for cropland across the world[6] for A2 and B1 scenarios for the period 2000-2050. The panel (a) of this figure indicates that in the scenario A2 the demand for cropland has an increasing trend until 2035 and thereafter it follows a decreasing trend in all regions across the world. This scenario predicts that the demand for cropland will be increased significantly in South East Asia, Former Soviet Union, and South America regions. The panel (b) of figure 2 indicates that the demand for cropland under the scenario B2 follows a different pattern across the world. In this scenario, the demand for cropland follows a decreasing trend in all regions, except for South East Asia and the Former Soviet Union regions. In these two regions the demand for cropland has an increasing trend until 2030 and it follows a decreasing trend in both regions thereafter.

In addition to the demand for cropland, humans need land for urbanization purposes. We determine urban land use changes according to the predicted population for each grid zone and a density rule. Grubler et al. (2006) have predicted spatial distribution of population for the time period 1900 to 2100 at the grid zone level (0.5^{o} by 0.5^{o}) for three IPCC scenarios: A1, A2, and B1. We used their predictions for A2 and B1 scenarios for the time period of 2000-2050. For the density rule we followed Waggoner (1994)[7], which assumes $F = a(D)^{\beta}$. Here F and D represent fraction of land in urban use and population density in each grid zone, respectively and a and β are constant parameters. Following his estimates we used values of $a = 0.046$ and $\beta = 0.866$ for all grid zones.

We used the downscaling method, which is discussed above, to distribute changes in the regional demands for cropland and urbanization across grid zones.

---

[5] For brief description of the MiniCAM model see: http://www.pnl.gov/gtsp/research/minicam.stm

[6] Here the world is divided into 7 regions: North America, Latin America, West Europe (WEUR), Africa, South East Asia (SE Asia), Former Soviet Union (FSU), Rest of the World.

[7] Available on line at: http://www-formal.stanford.edu/jmc/nature/nature.html

3. Data

The climate data for both scenarios (A2 and B1) is taken from the National Center for Atmospheric Research (NCAR)'s Community Climate System Model, version 3 (CCSM3) data, supported by the Directorate for Geosciences of the National Science Foundation and the Office of Biological and Environmental Research of the U.S.[8] The Land and Water Development Division of Food and Agriculture Organization of the United Nations and the Johann Wolfgang Goethe University have developed a digital map which shows areas equipped for irrigation. We used this map to adjust the LGP for Irrigated areas[9]. In addition, we assume irrigated areas remain unchanged in the future. Fischer et al., (2000) have provided the map of the global terrain slope with a resolution of 5 arc minute. We convert this map to a 0.5 degree resolution. Grubler et al. (2006) have predicted spatial distribution of population for the time period 1900 to 2100 at the grid zone level (0.5^{o} by 0.5^{o}) for three IPCC scenarios: A1, A2, and B1. We used their predictions for A2 and B1 scenarios for years 2000 and 2050. The historical land use change data are taken from Jain and Yang (2005). They provide two historical land use data sets: RF, a land use data set based on Ramankuty and Folley (1998, 1999) and HH, a land use data set based on Houghton and Hackler (1999). In this paper we used the RF data set.

4. Results

4.1. Urban Land Use

Map 1 panels (a) and (b) show changes in the demand for urban land across the world for scenarios A1 and B2, respectively. The panel (a) shows that under the scenario A2, the demand for urban land will increase across the world. In particular, a major increase in the demand for urban land will be accrued in the south and east of Asia, central region of Africa, and Latin America. The panel (b) of map 1 shows that under the scenario B1 the demand for urban land will not increase significantly in many of regions across the world. The exceptions are South East Asia, Africa, Middle East, and Latin America.

---

[8] This data is available at: http://eos-webster.sr.unh.edu/data/SR.jsp

[9] This map is available at: http://www.fao.org/ag/agl/aglw/aquastat/irrigationmap/index.stm

4.2. The LGPs

Map 2 shows the LGP for 2000. Results are, in general, consistent with previous studies in global agro-ecological zoning (AEZ) (for example, see Fischer et al., 2000 and Lee et al. (2005)). Map 3 panels (a) and (b) show changes in the LGP between 2000 and 2050 for both scenarios of A2 and B1, respectively. While these panels represent relatively similar patterns of changes for the LGP, a careful examination of the results reveals significant differences between changes in the LGP under scenarios A2 and B1. For example, while the panel (a) shows that the LGP will increase significantly in north and west of North America, the panel (b) depicts a moderate changes in these areas. As an another example, while the panel (a) represents a significant decrease in the LGP in the central area of the South America, the panel (b) shows a few changes in this region. In general, one can see that the A2 scenario causes more changes in the LGP across the world compared to the B1 scenario. To further examine these results, following Lee et al. (2005), we divide the world along the humidity gradients into 18 AEZ categories. We then derive land area according to these classes over time. Results are depicted in table 1. These results indicate that more land will be available for AEZs which represent a LGP between 120 to 239 days in the future under both scenarios.

4.3. Distribution of Cropland Changes across the World

Map 3 panels (a) and (b) show distribution of cropland changes across the world between 2000 and 2050 for scenarios A2 and B1, respectively. The panel (a) indicates that the Midwest area in the North America, central area towards east in the Former Soviet Union (FSU) region, central area towards east in Africa, and south of the SEA will provide more croplands under the scenario A2. The panel (b) shows that there will be reductions in the demand for cropland in several regions across the world, including central area towards west in the North America, east and west of South America, central area in Africa, and east of SEA under scenario B1. These are representing marginal land in each region, in general.

4.4. Forestation and Deforestation across the World

Map 4 panels (a) and (b) show distribution of forest land changes across the world between 2000 and 2050 for scenarios A2 and B1, respectively. The panel (a) indicates that deforestation will accrue mainly in the North America, Europe, FSU and SEA under the scenario A2. In theses regions forests will be transferred to crop land and urban land to cover human needs. The panel (b) shows a mix of deforestation and reforestation across the world under the scenario B1.

4.4 Emissions from Land Use Changes

Table 2 shows that under the A2 scenario land use changes generate considerable amount of emissions for CO2 and reactive GHGs (CO, NMHCs, and NOx). In general, emissions under this scenario follow an increasing pattern during the time period 2000-2035 and then they track a decreasing trend towards the end of the 2050s,. For example, CO_2 from land uses changes rises from 0.4 Gt/yr in 2000 to 0.8 Gt/yr in 2025, and then it falls to 0.6 Gt/yr in 2050. Table 2 also shows that land use changes generate consider amount of reactive GHGs. Under this scenario land use changes generate 71.1 Tg/yr CO, 1.9 Tg/yr No_x, and 4.9 Tg/yr NMHCs in 2025. These emissions drop to 16.5 Tg/yr, 0.4 Tg/ye, and 1.0 Tg/yr in 2050, respectively. Under scenario B1 land use changes do not contribute to emissions. Under this scenario land use changes generate 0.4 and 0.3 Gt/yr CO_2 in 2025 and 2050, respectively.

5. Conclusions

This paper has evaluated the potential contribution of regionally-specific land use-related activities to the future emissions at 0.5^o x 0.5^o resolution. It has developed a framework which spatially disaggregates future land uses changes based on socio-economic, biophysical, and biogeochemical factors at 0.5^o by 0.5^o resolution. The emissions are calculated using the developed downscaling framework for two IPCC scenarios (A2 and B1). Results indicate that these two scenarios generate two different patterns of land use changes across the world. The A2 scenario will cause a major land use changes and leads to a considerable amount of emissions from land use changes. The B2 scenario does not affect future land use significantly and hence it does not emit emissions from land use changes. Results also show that Agro-Ecological zones (AEZs) are changing over time as a result of changes in biophysical and biogeochemical factors over time. In general, results also indicates that more land will be available for the AEZs which represent a length of growing period between 120 to 239 days in the future under both scenarios, in particular for the A2 scenario.

Acknowledgements

This research was supported in part by the Office of Biological and Environmental Research (OBER), U.S. Department of Energy (DOE-DE-FG02-06ER64195).

References

Eickout, B., H. van Meijl and A. Tabeau, (2008). "The impact of Environmental and Climate Constraints on Global Food Supply", In *Economic Analysis of Land Use in Global Climate Change Policy*. Edited by T. Hertel, S. Rose and R. Tol. Routledge: forthcoming.

Feddema, J., K. Oleson, G. Bonan, L. Mearns, L. Buja, G. Meehl, and W. Washington, (2005). "The Importance of Land-Cover Change in Simulating Future Climates", *Science* 9 December 2005: Vol. 310. no. 5754, 1674 – 1678.

Fischer, G., H. van Velthuizen, F. Nacgtergaele, and S. Medow, (2000). *Global Agro-Ecological Zones (Global-AEZ)*, Food and Agricultural Organization (FAO) of the United Nation (UN) and Intrenatinal Institute fro Applied System Anaysis (IIASA).

Fischer, G., H. van Velthuizen,S. Medow , F. Nachtergaele, (2002). *Global Agro-Ecological Assessment for Agriculture in the 21st Century: Methodology and Results* (Research Report RR-02-02). Laxenburg, Austria: International Institute for Applied Systems Analysis (IIASA) and Food and Agriculture Organization (FAO) of the United Nations (UN).

Grubler A., B. O'Neill, K. Riahi, V. Chirkov, A. Goujon, P. Kolp, I. Prommer, S. Scherbov, and E. Slentoe, (2006). "Regional, national, and spatially explicit scenarios of demographic and economic change based on SRES", Technological Forecasting & Social Change, In Press.

Houghton, R.A., (2003). "Revised estimates of the annual net flux of carbon to the atmosphere from changes in land use and land management: 1850-2000", *Tellus Series B-Chemical and Physical Meteorology, 55* (2), 378-390.

Houghton, R. A., and J. L. Hackler (1999), Emissions of carbon from forestry and land-use change in tropical Asia, Global Change Biol., 5, 481– 492.

Jain, A.K., Z. Tao, X. Yang, and C. Gillespie, (2006). "Estimates of global biomass burning emissions for reactive greenhouse gases (CO, NMHCs, and NOx) and CO2", *Journal of Geophysical Research*, Vol. 111, D06304, 1-14.

Jain, A.K. and X. Yang, (2005). "Modeling the Effect of Two Different Land Cover Change Data Sets on the Carbon Stocks of Plants and Soil in Concert with CO_2 and Climate Change", *Global Biogeochemical Cycle*, Vol. 19, GB2015, 1-20.

Lee H., T. Hertel, B. Sohngen, and N. Ramankutty, (2005). "Towards An Integrated Land Use Data Base for Assessing the Potential for Greenhouse Gas Mitigation", GTAP Technical Paper No. 25.

Nakicenovic, N. and R. Sward, (2000). *Emission Scenarios,* Special Report of the Intergovernmental Panel on Climate Change, Cambridge, UK: Cambridge University Press.

Ramankutty, N., and J. Foley (1998). “Characterizing patterns of global land use: An analysis of global croplands data”, *Global Biogeochem*. Cycles, 12(4), 667– 685.

Ramankutty, N., and J. A. Foley (1999). “Estimating historical changes in global land cover: Croplands from 1700 to 1992”, *Global Biogeochem*. Cycles, 13(4), 997–1027.

Rokityanskiy D., P. Benitez F. Kraxner, I. McCallum, M. Obersteiner, E. Rametsteiner, Y. Yamagat, (2006). “Geographically explicit global modeling of land-use change, carbon sequestration, and biomass supply”, Technological Forecasting & Social Change, In Press.

Rotmans, J., (1990). “IMAGE: An Integrated Model to Assess the Greenhouse Effect”, Proefschrift, Kluwer Academics, Dordrecht, The Netherlands. 39, 45.

Rounsevell, M.D.A., F. Ewert, I. Reginster, R. Leemansc, and T.R. Carter, (2005). “Future scenarios of European agricultural land use II. Projecting changes in cropland and grassland”, *Agriculture, Ecosystems and Environment* 107 (2005) 117–135.

Tian, H., J. M. Melillo, D. W. Kicklighter, et al., (1999). “The Sensitivity of Terrestrial Carbon Storage to Historical Atmospheric CO_2 and Climate Variability in the United States”, *Tellus*, 51B:414-452.

Verburg P., G. de Koning, K. Kok; A. Veldkamp, and J. Bouma, (1999). “A spatial explicit allocation procedure for modelling the pattern of land use change based upon actual land use”, *Ecological Modelling*, Volume 116, Number 1, 1 March 1999, pp. 45-61(17).

Waggoner, E., (1994). “How much land can ten billion people spare for nature?”, Task Force Report, No. 121 February 1994.

Figure 1. Schematic diagram of the terrestrial ecosystem component of the Integrated Science Assessment Model

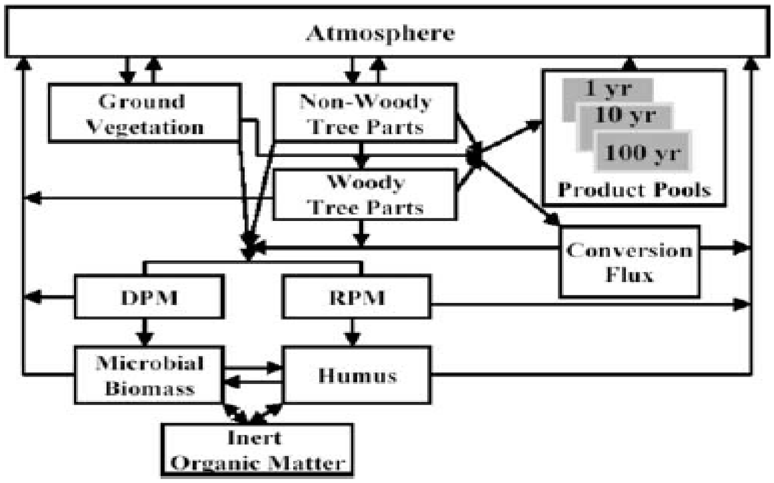

Figure 2. Demand for Cropland (2000-2050)

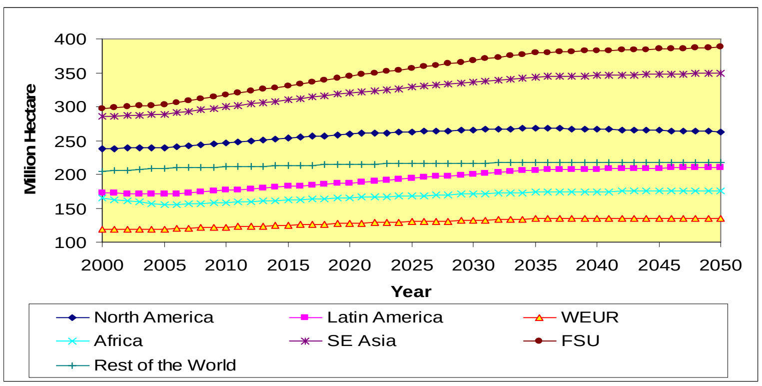

Panel (a). Scenario A2

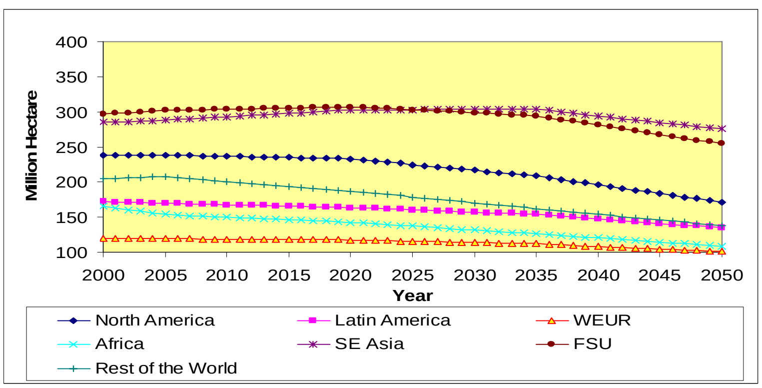

Panel (b). Scenario B1

Map 1. Urban Land Use Changes across the World

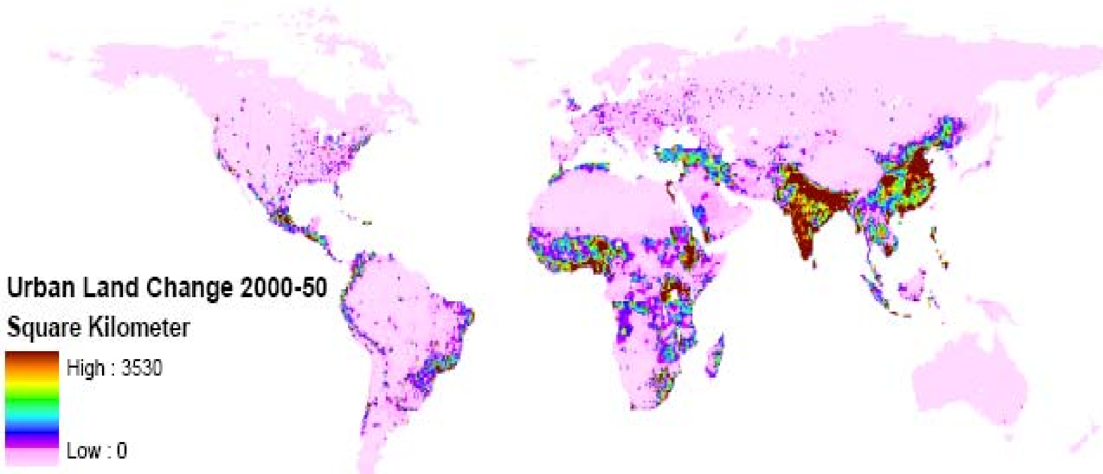

Panel (a). Scenario A2

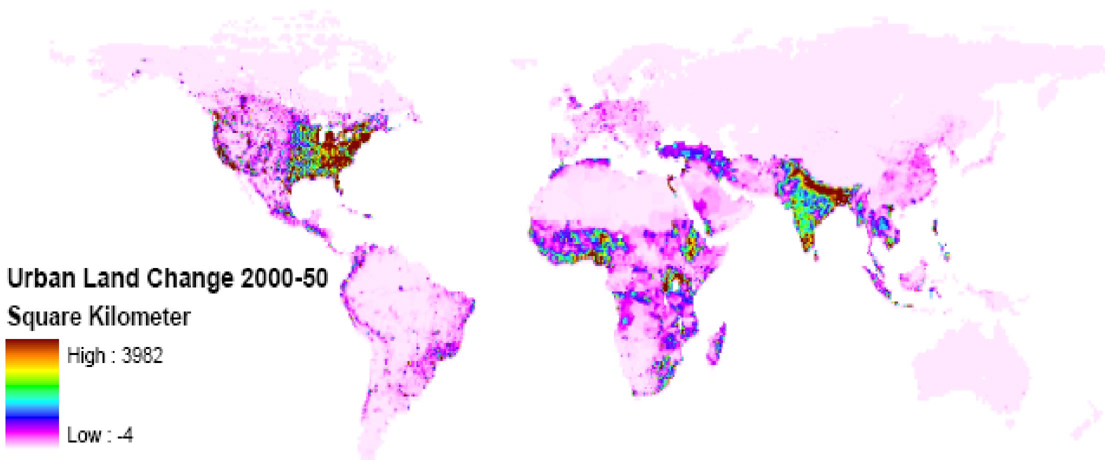

Panel (b). Scenario B1

Map 2. Length of Growing Period 2000

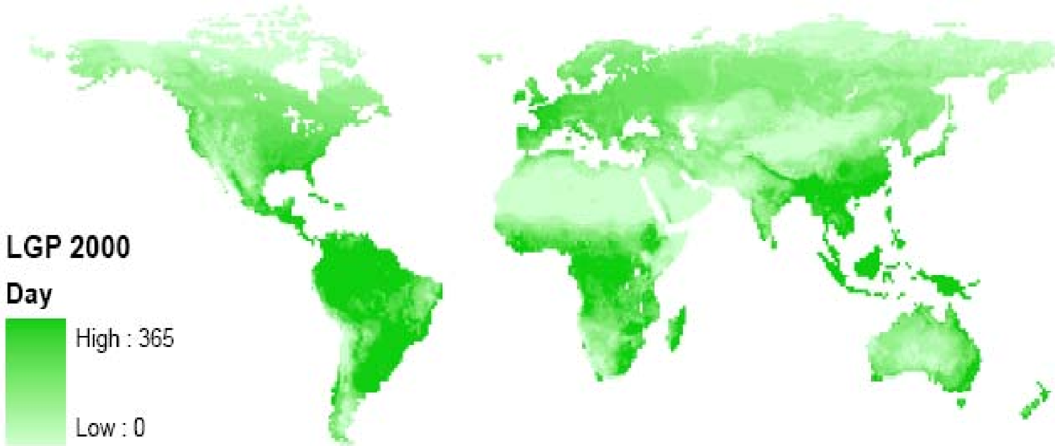

Map 3. Change in the Length of Growing Period 2000-50

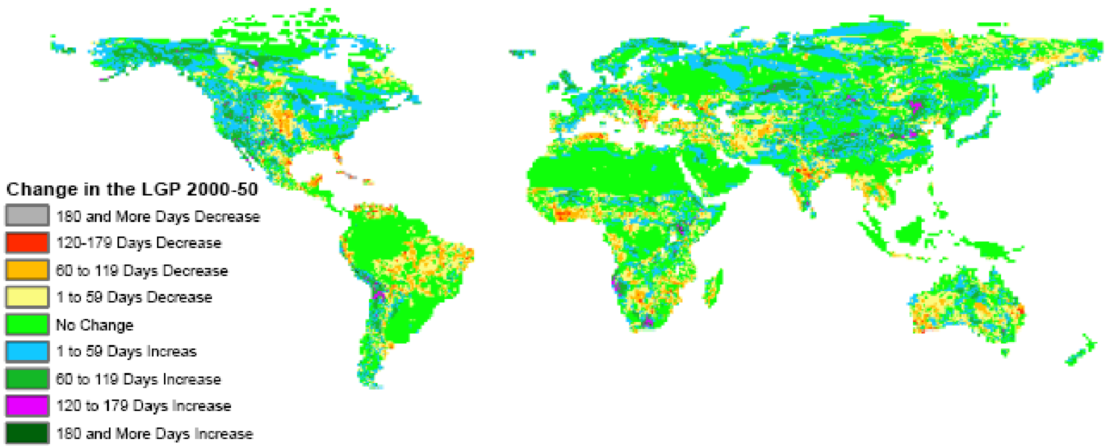

Panel (a). Scenario A2

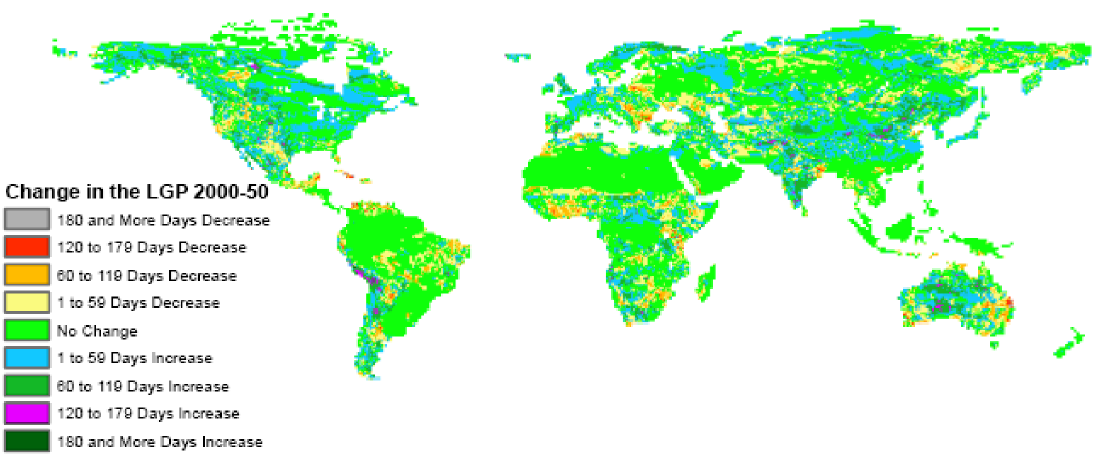

Panel (b). Scenario B1

Map 4. Distribution of Cropland Changes across the World (2000-2050)

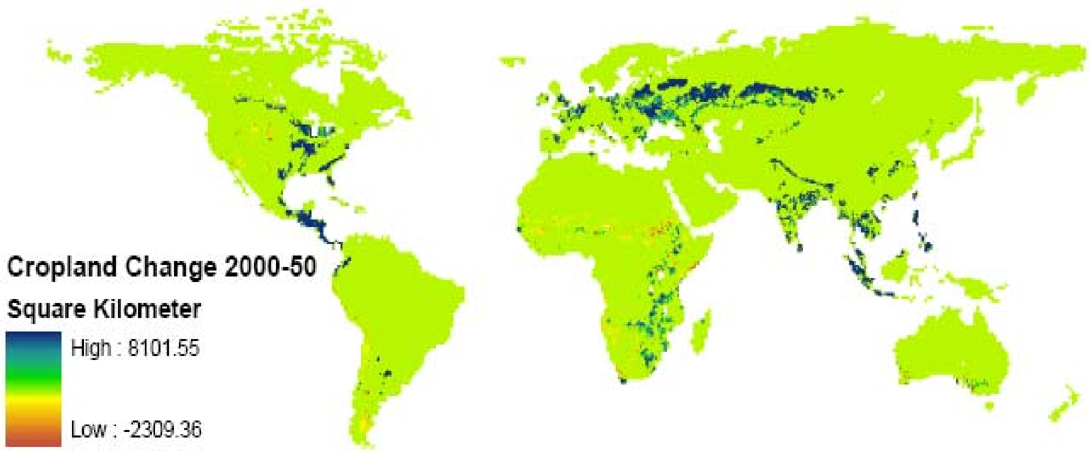

Panel (a). Scenario A2

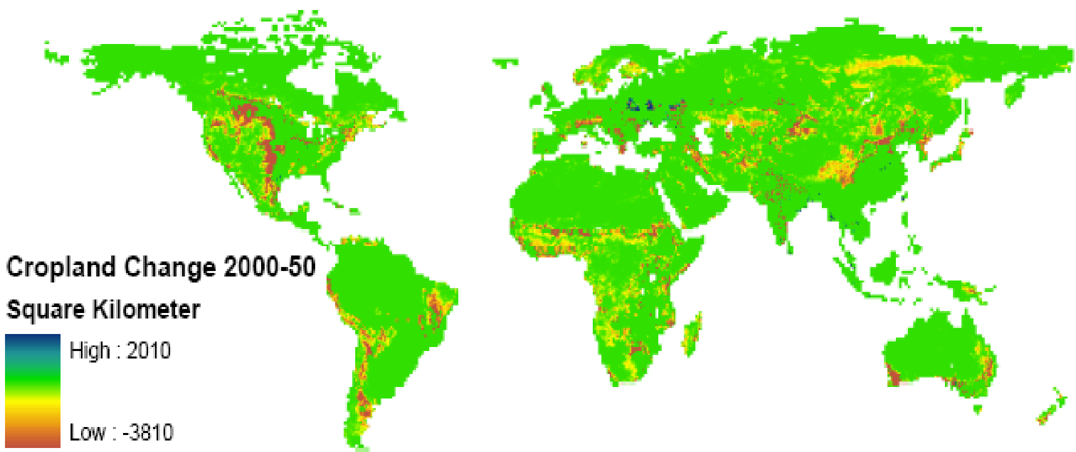

Panel (b). Scenario B1

Map 5. Distribution of Forest Area Changes across the World (2000-2050)

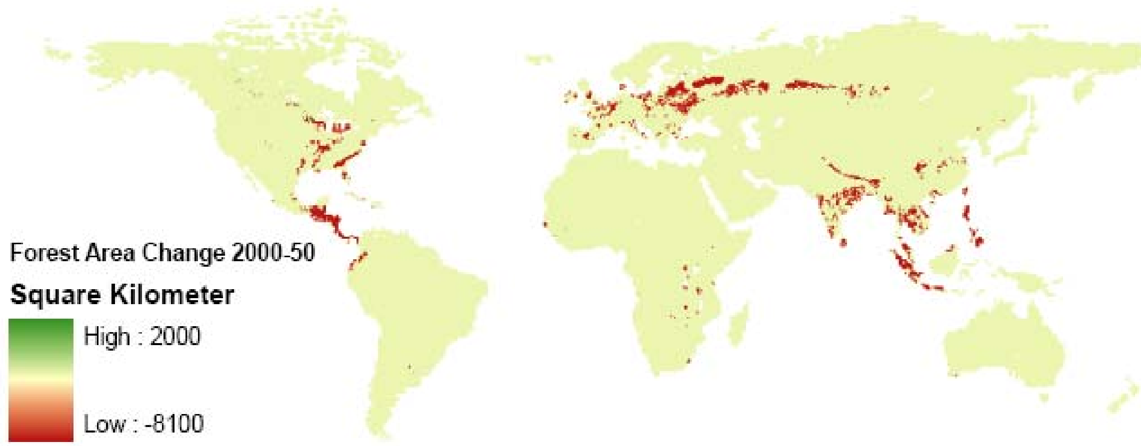

Panel (a). Scenario A2

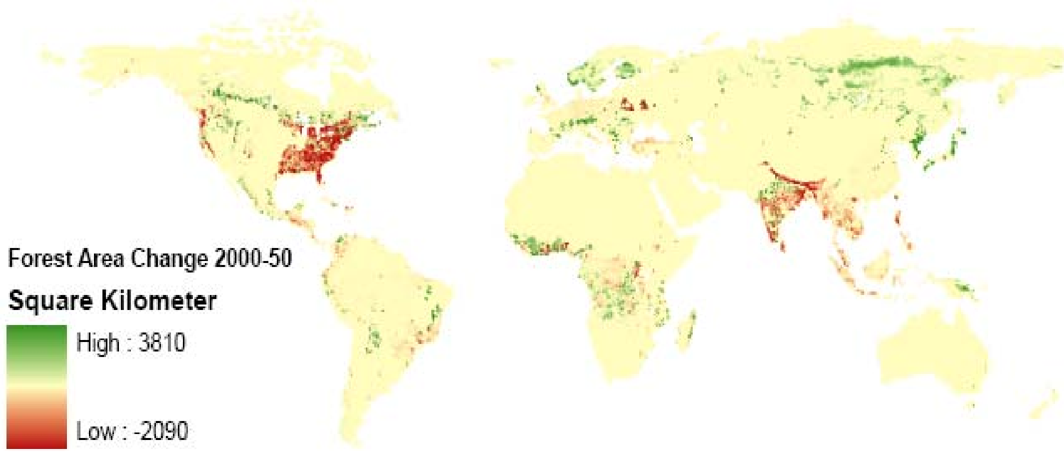

Panel (b). Scenario B1

Table 1. Distribution Land across AEZs in 2000 and 2050

AEZ	LGP	A2 Scenario		B1 Scenario	
		2000	2050	2000	2050
AEZ1, AEZ7, AEZ13	0-59	22.8	21.5	22.8	20.9
AEZ2, AEZ8, AEZ14	60-119	14.7	13.8	14.7	13.4
AEZ3, AEZ9, AEZ15	120-179	17.6	18.1	17.6	18.1
AEZ4, AEZ10, AEZ16	180-239	12.7	15.0	12.7	15.4
AEZ5, AEZ11, AEZ17	240-299	8.3	9.0	8.3	8.1
AEZ6, AEZ12, AEZ18	300 and more	23.9	22.6	23.9	24.0
Total		100.0	100.0	100.0	100.0

Table 2. Land Use Change Greenhouse Gasses

Greenhouse Gases	A2 Scenario			B1 Scenario		
	2000	2025	2050	2000	2025	2050
CO_2 (Gt/yr)	0.4	0.8	0.6	0.4	0.4	0.3
CO (Tg/yr)	56.2	71.1	16.5	56.2	-	-
NOx (Tg /yr)	1.3	1.9	0.4	1.3	-	-
NMHCs (Tg/yr)	4.0	4.9	1.0	4.0	-	-